Operational Optimization of an Agricultural Microgrid

Paul D. Brown

Department of Electrical and Electronics Engineering
Middle East Technical University
Ankara, Turkey
ORCID: 0000-0001-5753-0449

Murat Göl

Department of Electrical and Electronics Engineering
Middle East Technical University
Ankara, Turkey
ORCID: 0000-0002-2523-1169

Abstract—A demonstration agricultural microgrid containing solar photovoltaic (PV), battery storage system (BSS) and multiple water pumps and reservoirs is presented. A mathematical model of the cost of operating the demonstration microgrid is developed. The mathematical model includes hybrid inverter source switching and BSS charging modes in addition to power balance and inter-period energy and water-level coupling. Electricity pricing and irrigation water use efficiency are allowed to vary by time of day. The mathematical model is formulated as a mixed-integer linear program (MILP), implemented in Python using Pyomo, and optimized using the open-source CBC solver to plan pumping and water usage. Estimated data for a demonstration system at a farm in Turkey is used to demonstrate the proposed model. Results of the optimization of the demonstration system show intuitive results that are superior to a rule-based initialization. The model may serve as the basis for model predictive control (MPC) or stochastic model predictive control (SMPC).

Index Terms—Microgrid, optimization, photovoltaic systems, energy storage, irrigation

I. INTRODUCTION

Many factors are driving change within the electrical power industry over recent decades. One such trend is the ongoing electrification of rural regions around the globe. For agricultural consumers, electrification enables increased yields and economic development. Ref. [1] reviews technology and applications for off-grid systems for rural electrification.

Use of solar photovoltaic (PV) and other renewable distributed energy resources (DER) facilitates rural electrification by reducing the infrastructure cost required. PV energy is generally well aligned with water needs[2]. Ref. [2] reviews numerous solar-powered water pumping applications around the world while [3] reviews the PV and water pumping modeling, design, and control approaches in the literature.

In recent years, much research has been done into the benefits and issues related to microgrids[4, 5]. While microgrids can facilitate rural electrification by allowing connection of loads and distributed energy sources with or without a connection to the main grid, development of microgrids requires new techniques for planning, control, and operation[6, 7].

Much of the literature regarding optimization of microgrids has focused on design optimization and optimal sizing of system components[6, 8]. Ref. [9] investigates the optimal operation of a microgrid including pumped hydro energy storage by formulating a non-linear optimization problem

and using the two-point estimate method (TPEM) to account for uncertainty. In [10], the authors evaluate three rule-based control strategies using the HOMER Pro microgrid analysis tool. Ref. [11] proposes a MPC for battery energy storage system (BESS) associated with a grid-connected PV system. The proposed control scheme determines the BESS power schedule, maximizing profit from real-time energy price arbitrage by time-shifting while accounting for BESS costs associated with cycling and smoothing the plant and BESS output.

This paper focuses on the operational planning of an agricultural microgrid with a grid connection, a DER (PV), irrigation pumping load, and water and electrical energy storage. This paper presents an original mathematical formulation of the operational optimization problem suitable for model-predictive control (MPC) of an agricultural microgrid. The novelty of this work is the inclusion of PV and water needs as well as the modeling of the hybrid inverter source switching and BSS charging modes.

In this paper, Section II briefly describes the demonstration system that is modeled. Then in Section III, the mathematical formulation of the problem is presented. Data used for the demonstration system is shown in Section IV. Implementation details are provided in Section V. In Section VI, results of the optimization for the demonstration system data is shown. Section VII describes some conclusions and directions for future work.

II. DEMONSTRATION SYSTEM

The optimization problem is specifically formulated for a demonstration system to be installed at the Güneşköy farm[12]. A block diagram of the demonstration system with anticipated component ratings is shown in Fig. 1.

The existing pump will continue to be fed from the grid. The site electrical load will be fed from a hybrid inverter[13] that will have battery, PV, and grid connections available. A new pump load will be fed from an inverter drive[14] connected to the PV DC bus.

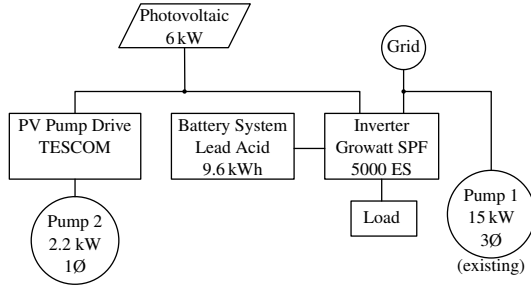The power flow directions within the demonstration system are shown in Fig. 2.
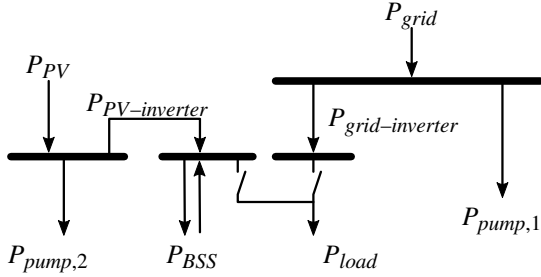
Fig. 1. Güneşköy Demonstration System

Fig. 2. Microgrid power flows

III. PROBLEM FORMULATION

The problem variables, objective function, and constraints are described in the following subsections. Refer to Tables I to III for definitions of the symbols used.

A. Problem variables

The problem variables are shown in Table I. The optimization determines the best times to run Pump 1, when and how much to run Pump 2, and when to utilize water for irrigation.

B. Objective function

The objective function includes several components and is shown in (1). The actual cost component is the cost of grid power. The cost of battery usage component represents the portion of the replacement cost of the battery system incurred due to the loss of life caused by battery cycling[15]. The other penalty factors encourage the full supply of desired water on each day and discourage unnecessary switching of the BSS mode and Pump 1 respectively.

$$
\min \underbrace{\sum_t C_{grid,t}\, P_{grid,t}\, \Delta t}_{\text{Cost of grid power}}
$$
$$
+ \underbrace{\sum_t C_{BSS} \left(P_{BSS,ch,t} + P_{BSS,disch,t} \right) \Delta t}_{\text{Cost of battery usage}}
$$
$$
+ \underbrace{C_{w,short} \sum_d \max \left(\left(V_{use,desired,d} - V_{use,d} \right), 0 \right)}_{\text{Penalty for inadequate water}}
$$
$$
+ \underbrace{C_{BSS,switching} \sum_t \left| s_{BSS,t} - s_{BSS,t-1} \right|}_{\text{BSS mode-switching penalty}}
$$
$$
+ \underbrace{C_{Pump1,switching} \sum_t \left| s_{pump1,t} - s_{pump1,t-1} \right|}_{\text{Pump 1 switching penalty}}
\tag{1}
$$

C. Constraints

The constraints represent mathematically the operation and allowable states of the microgrid system. The constraints related to each component of the microgrid are as follows:

TABLE III
PROBLEM PARAMETERS / DATA

Symbol	Description	Units
$P_{load,t}$	Power drawn by electrical loads	W
$P_{PV,avail,t}$	Power available from PV array (MPP)	W
$P_{pump1,max}$	Operating power of Pump 1	W
$s_{pump1,0}$	Initial state of Pump 1	-
Q_{w1}	Fixed water flow for Pump 1	m³/h
$P_{pump2,min}$	Minimum operating power of Pump 2	W
$P_{pump2,max}$	Maximum operating power of Pump 2	W
$Q_{w2}\left(P_{pump2}\right)$	Function relating pumped water quantity to electrical power for Pump 2	m³/h
$P_{BSS,ch,max}$	Bulk charging power for the BSS	W
$P_{BSS,disch,max}$	Maximum power for discharging the BSS	W
K_{BSS}	BSS absorption mode charge rate constant	-
$E_{BSS,0}$	Initial value of energy stored in the BSS	Wh
$s_{inv,0}$	Initial state of inverter	-
$E_{BSS,max}$	Maximum energy that can be stored in the BSS	Wh
$E_{BSS,lower}$	Inverter threshold to switch from BSS/PV source to utility source	W
$E_{BSS,upper}$	Inverter threshold to switch from utility source to BSS/PV source	W
$V_{w,r,0}$	Initial value of water stored	m³
$V_{w,r,min}$	Minimum volume of water	m³
$V_{w,r,max}$	Maximum volume of water	m³
$V_{use,desired,d}$	Desired volume of effectively used water on day d	m³
D_d	Set of time periods t belonging to day d.	-
$Q_{use,r,max}$	Maximum rate of water use	m³/h
$C_{grid,t}$	Cost of power from the grid	\$/Wh
C_{BSS}	Cost of storing power in the BSS	\$/Wh
$C_{BSS,switching}$	Penalty for changing BSS charging/discharging mode	\$/ea
$C_{w,short}$	Cost or penalty factor for water that is desired but not used	\$/m³
η_{BSS}	Efficiency of BSS in charging or discharging	-
$\eta_{w,t}$	Efficiency of water use	-
Δt	Time interval for discretized planning horizon	h

[1] Parameters subscripted with t have a value for each time period
[2] Parameters subscripted with r have a value for each reservoir

1) Power Balance: There is a power balance constraint equation for each of the four buses shown in Fig. 2. Equation (2) enforces balance on the PV bus, (3) enforces balance in the hybrid inverter PV/BSS side, (4) enforces balance in the hybrid inverter grid side, and (5) enforces balance on the grid-side bus.

$$P_{PV,t} - P_{pump2,t} - P_{PV-inverter,t} = 0 \qquad (2)$$

$$\begin{aligned} P_{PV-inverter,t} + P_{BSS,disch,t} - P_{BSS,ch,t} \\ - \left(1 - s_{inv,t}\right) P_{load,t} = 0 \end{aligned} \qquad (3)$$

$$P_{grid-inverter,t} = s_{inv,t}\, P_{load,t} \qquad (4)$$

$$P_{grid,t} - P_{grid-inverter,t} - P_{pump1,t} = 0 \qquad (5)$$

The direction of power flow from the PV bus to the inverter and from the grid to the inverter are constrained to be positive as shown in (6) and (7).

$$0 \leq P_{PV-inverter,t} \qquad (6)$$

$$0 \leq P_{grid-inverter,t} \qquad (7)$$

2) Photovoltaic: It is assumed that the microgrid has the ability to track the photovoltaic array maximum power point (MPP) regardless of the operation of either or both of the hybrid inverter and the drive for Pump 2. It is also assumed that the control system has the ability to know what the maximum available PV power is, even if the system is not operating at the MPP. The full available output of the PV system may not be used if the load is less than the available PV power.

$$0 \leq P_{PV,t} \leq P_{PV,avail,t} \qquad (8)$$

3) Pumps: Pump 1 is operated in a simple on-off fashion at a fixed power level.

$$P_{pump1,t} = s_{pump1,t}\, P_{pump1,max} \qquad (9)$$

$$Q_{pump1,t} = s_{pump1,t}\, Q_{w1} \qquad (10)$$

It is assumed that Pump 2 may be operated at a specified range-limited power setpoint chosen by the controller. The pumping power $P_{pump2,t}$ is a semi-continuous variable, being continuous between a minimum and a maximum or else 0.

$$P_{pump2,t} = 0 \;\lor\; P_{pump2,min} \leq P_{pump2,t} \leq P_{pump2,max} \qquad (11)$$

$$Q_{pump2,t} = Q_{w2}\left(P_{pump2,t}\right) \qquad (12)$$

Equation (13) is a placeholder for the currently unknown relationship between pump flow and power. For real-time control, the EMS controller could infer this relationship by observing the operation of the pump. Until then, a simple linear efficiency coefficient η_{pump2} is used to characterize the power-flow relationship of Pump 2.

$$Q_{w2}\left(P_{pump2,t}\right) = \frac{P_{pump2,t}\, \eta_{pump2}}{h\rho g} \qquad (13)$$

4) Hybrid Inverter and BSS: The hybrid inverter selected for the demonstration system at Güneşköy has limited capability to receive external control. It is assumed that the hybrid inverter will be configured with a priority order for supplying load such that the load will be supplied from PV if available, supplemented by power from the BSS. If PV is not sufficient and the BSS charge level is too low, then the utility grid source will be used. It is assumed that the hybrid inverter will charge the BSS only from PV and not from the utility grid source.

It is planned for the BSS to consist of lead-acid batteries. The hybrid inverter is responsible for charging the lead-acid battery bank. The inverter uses a four-stage charging cycle[14]:

1) **Bulk charging.** Charges at a settable maximum charging current. The power to the battery is nearly constant and is approximated in this formulation as a constant power $P_{BSS,ch,max}$.

2) **Absorption charging.** Once the voltage reaches the set maximum charging voltage, the voltage is held for a duration of 10 times the time spent in bulk charging mode. The power to the battery declines exponentially with time as the BSS voltage approaches the charging voltage and the SOC approaches 100%.

3) **Float charging.** Once the absorption charge timer completes, the charger switches to float charging mode in which a fixed voltage is held and minimal charging current

is output except to compensate the small battery internal discharge or load discharging of the battery.

4) **Equalization charging.** Equalization charging is only applicable to flooded lead acid batteries and not to sealed lead acid batteries. In this mode, the battery is temporarily overcharged in order to reduce sulfation on the battery plates.

For the purposes of a mathematical model of the hybrid inverter's battery charging system for this optimization problem, only the bulk charging and absorption charging modes are represented. The other charging modes are neglected since most of the energy transfer to the BSS is completed these modes.

Equation (14) forces the charger state to charging mode if power is available. Equation (15) enforces the limit for absorption charging mode of the hybrid inverter, limits charging power to available power from the PV after meeting pumping and load power, and only allows charging when $s_{BSS,t}$ is in charging mode. Equation (16) only allows discharging when $s_{BSS,t}$ is in discharging mode.

$$s_{BSS,t} = \left(P_{PV,avail,t} - P_{pump2,t} - (1 - s_{inv,t})P_{load,t} \geq 0 \right) \quad (14)$$

$$P_{BSS,ch,t} = \min \Bigg(\underbrace{K_{BSS} \ \frac{E_{BSS,max} - E_{BSS,t-1}}{\eta_{BSS} \ \Delta t}}_{\text{Absorption mode charging limit}},$$

$$\underbrace{P_{PV,avail,t} - P_{pump2,t} - (1 - s_{inv,t})P_{load,t}}_{\text{Unused available PV power}}, \quad (15)$$

$$\underbrace{s_{BSS,t} \ P_{BSS,ch,max}}_{\text{Enforce charger mode}} \Bigg)$$

$$0 \leq P_{BSS,disch,t} \leq \left(1 - s_{BSS,t}\right) P_{BSS,disch,max} \quad (16)$$

The constant K_{BSS} takes a value between 0 and 1 and determines this switchover point from bulk charging mode to absorption charging and the rate of decrease in the charging power in absorption charging mode. A K_{BSS} value of 1 indicates that the charger remains in bulk charging mode until the BSS is fully charged. The value of K_{BSS} can be related to the time constant of the exponential decay of charging power in absorption mode, τ_{BSS}, as shown in (17). This relationship can be used to calculate K_{BSS} or to convert a known K_{BSS} from one modeling time interval Δt to another.

$$K_{BSS} = 1 - e^{-\Delta t/\tau_{BSS}} \quad (17)$$

According to the the hybrid inverter user manual[14], when in "SBU priority" mode, the hybrid inverter switches from PV/battery source to utility source when the battery goes below a minimum voltage level and switches back to the battery when the battery rises above a minimum voltage level. Equation (18) represents this logic to determine the connection of the inverter in time period t based on the connection during the previous period and the BSS energy level at the end of the previous period. Modeled this way, the mode is switched only at discrete time intervals, so the model will show the battery BSS charge level will going a little above and below the set thresholds

rather than switching mid-period as the actual hybrid inverter will do.

$$s_{inv,t} = \left(s_{inv,t-1} \text{ and } \left(E_{BSS,t-1} \leq E_{BSS,upper} \right) \right) \text{ or } \\ \left(E_{BSS,t-1} \leq E_{BSS,lower} \right) \quad (18)$$

Equation (19) couples the battery system energy balance from one period to the next. It includes a factor for conversion losses on energy input and energy output. An alternative formulation would be to make the efficiency factor be "round trip" and only include it on one of charging or discharging power rather than both.

$$E_{BSS,t} = E_{BSS,t-1} + P_{BSS,ch,t} \ \eta_{BSS} \ \Delta t - \frac{P_{BSS,disch,t} \ \Delta t}{\eta_{BSS}} \quad (19)$$

5) Water Flow: Equation (20) couple the water level in the reservoirs from one period to the next.

$$V_{w,r,t} = V_{w,r,t-1} + Q_{pump,r,t} \ \Delta t - Q_{use,r,t}\Delta t \quad (20)$$

Equation (21) sums the effective irrigation water across periods in each day, taking into consideration the varying efficiency of irrigation in different periods. It is assumed that water use between the reservoirs is interchangeable.

$$V_{use,d} = \sum_{t \in D_d} \sum_r \eta_{w,t} Q_{use,r,t} \Delta t \quad (21)$$

Equations 22 and 23 are the limits on feasible values of the water flow and reservoir level values.

$$0 \leq Q_{use,r,t} \leq Q_{use,r,max} \quad (22)$$

$$V_{w,r,min} \leq V_{w,r,t} \leq V_{w,r,max} \quad (23)$$

IV. DATA VALUES

Data for the problem parameters was estimated based on the planned demonstration system shown in Fig. 1. While the parameters used are intended to represent a realistic system, they have not been validated operationally.

Grid energy costs $C_{grid,t}$ were set for the daytime, peak, and nighttime rates and daily periods that Güneşköy was billed at in 2020, not including fees for power factor, etc.

Water usage efficiency $\eta_{w,t}$ was set using different values for each hour of the day, with the highest efficiency (1.0) during nighttime hours and the lowest efficiency (0.5) during early afternoon.

Random values were generated for the load and the desired water use. Load was drawn from a uniform distribution ranging from 0 to 1 kW. Daily desired water use was drawn from a normal distribution with a mean of 70 m^3 and a standard deviation of 30 m^3.

Pump, battery, and PV parameters were selected to represent the demonstration system shown in Fig. 1. The hybrid inverter source selection was configured to stay on the PV/BSS source until the BSS charge dropped below 30% and then switch to the grid to charge until it reached a charge level of 95%. The BSS charging and discharging efficiency was set to 95%. Hourly averages of the recorded output power of the rooftop PV array on the METU EEE Department machinery building

	Initialized	Optimized
Grid energy cost	3826.2	2722.2
Battery use cost	292.1	341.6
Inadequate water cost	0.0	0.0
Battery mode switching cost	6.0	8.0
Pump switching cost	3.0	2.0
TOTAL	4127.3	3073.8

Fig. 3. PV-Side Power

Fig. 4. Grid-Side Power

were scaled to the rating of the demonstration system and used for the available PV power.

The optimization period was set for a length of 72 h with a time step Δt of 1 h used. The time period of 72 h (3 days) was used so that the optimizer wouldn't use up all the stored water and energy to meet the needs of the first day, neglecting its benefit for future days. Initial values for E_{BSS}, V_{w1}, V_{w2}, and s_{inv} were set arbitrarily for the first period optimized. For subsequent periods, the time period being optimized was slid forward by 24 h, and the value for the 24th hour of the previous period was used as the initial value for the current period. The results shown in Section VI are from the fourth in this series of sliding optimization runs.

V. IMPLEMENTATION

The problem was modeled in the Python programming language using the Pyomo library[16, 17] and solved using the COIN-OR CBC[18] open-source mixed-integer linear program (MILP) solver. In order to use a MILP solver, auxiliary binary variables were introduced to linearize non-linear functions such as max, min, absolute value, $\geq$, $\leq$, and logic functions and and or. The formulation of the non-linear functions was based on [19] and original work by the author. Details are provided in Appendix A. Semi-continuous variables were modeled using the approach described in [20].

The problem, solved for a time period of 72 h with an interval Δt of 1 h, contained a total of 566 continuous and 1008 binary variables. CBC converges to a solution in less than 30 seconds.

Initialization to a feasible point was performed using a single forward-pass heuristic of greedy pumping with Pump 2 if PV was available, then meeting loads with PV and BSS energy, discharging BSS to meet loads if necessarily and energy was available. Initial Pump 1 pumping and water use was set by iteratively solving a linear problem to try to add pumping one hour at a time until the desired water usage was met. The linear problem was implemented in Pyomo and solved using GLPK[21].

VI. RESULTS

The optimization run reduced the cost of the objective function from the initialized value of of 4127.3 to an optimized value of 3073.8. The components of the initialized and optimized objective function costs are shown in Table IV.

Fig. 3 shows the power on the PV and BSS side of the microgrid. Due to the relative ratings of the PV array, Pump
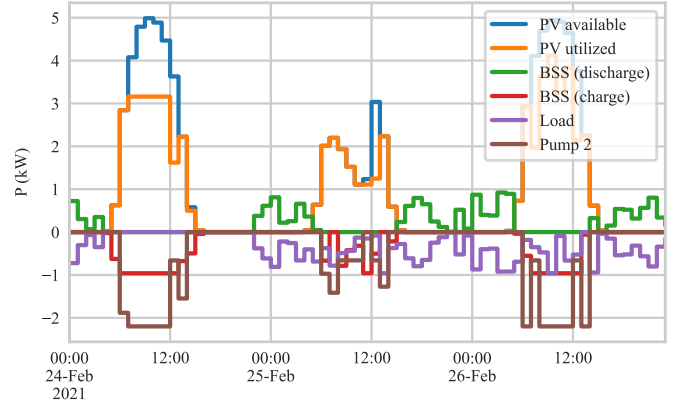
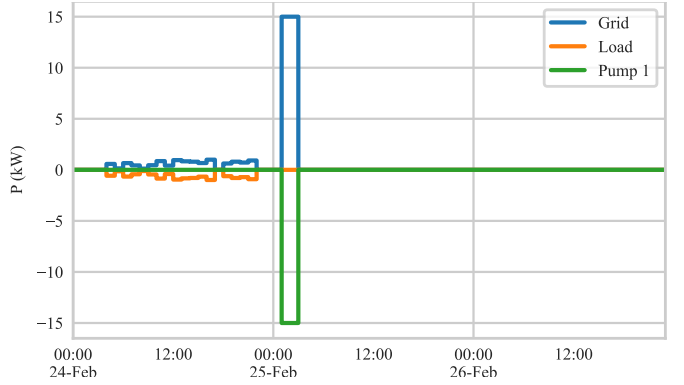2, and the BSS, on the sunny days (24 and 26 February), the full available PV power is not able to be used.

Fig. 4 shows the power on the grid side of the microgrid. On the first day (24 February), the hybrid inverter switches over to the grid because the BSS stored energy, shown in Fig. 5, is depleted before load can be met by power from the PV array, but once the BSS is recharged by PV during the day, the hybrid inverter switches back to the PV/BSS source and is able to supply the load for the rest of the modeled period. The largest load on the grid is Pump 1, which optimally runs during the nighttime hours where time-of-day electrical rates are cheapest.

Fig. 6 shows the charging and discharging power to the BSS. As one would expect, it follows a pattern of charging during the part of the day in which PV energy is available and discharging to meet load during the dark period.

Fig. 7 shows the water level in the two reservoirs while Fig. 8 shows the water usage from each reservoir throughout the day. Since the efficiency of water usage is highest at night, the optimal operation releases water during the nighttime hours.

VII. CONCLUSION

This paper has presented a detailed mathematical model for an agricultural microgrid suitable for optimization of the operation of the pumps and water usage. The model was
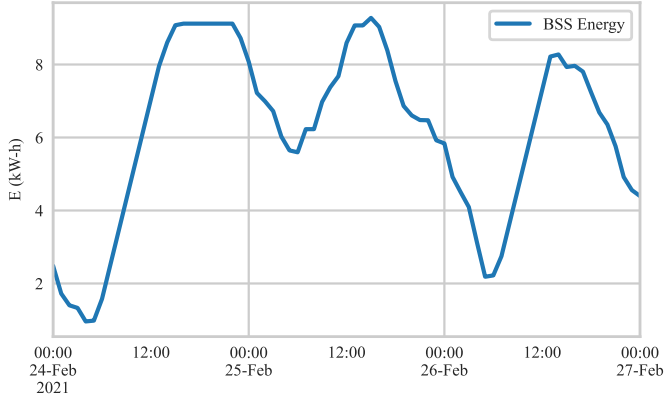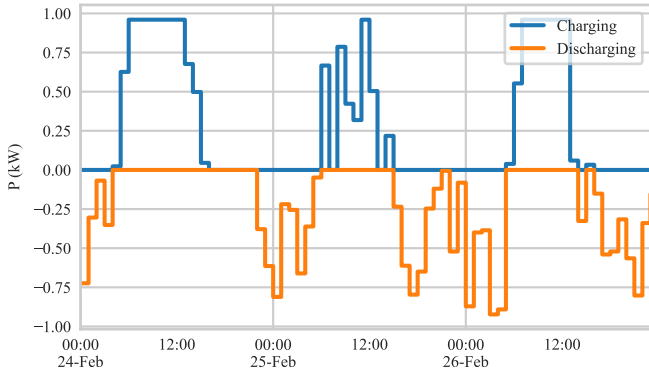
Fig. 5. BSS Energy Stored

Fig. 6. BSS Power (Charging & Discharging)

Fig. 7. Water Stored

Fig. 8. Water Used

implemented in open-source software and results have been presented.

The model is not intended to stand alone but to serve as one component of a microgrid energy management system (EMS). One possible application of this model is for use in model-predictive control (MPC) of the microgrid. In such a scheme, the system operation is optimized over some time horizon, but only the first step is used as the control output. The time horizon is then slid forward one step and the optimization is repeated.

In the formulation presented in this paper, a single value represents each of the parameters, including available PV power, loads, and desired water volume, all of which are dependent on random processes. One possible extension of this model would be to make it stochastic so that multiple possible future scenarios are represented. Unlike in standard MPC, where the output of the optimization problem is the control input (feed-forward), in stochastic model predictive control (SMPC), the output of the optimization problem is the optimal control law to be applied in the future time periods[22]. Thus, the system is able to respond to stochastic events dynamically without having to re-run the MPC problem to obtain new control outputs. A microgrid control system incorporating SMPC has been presented in [23].

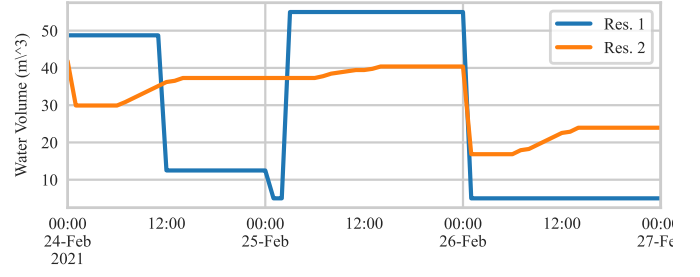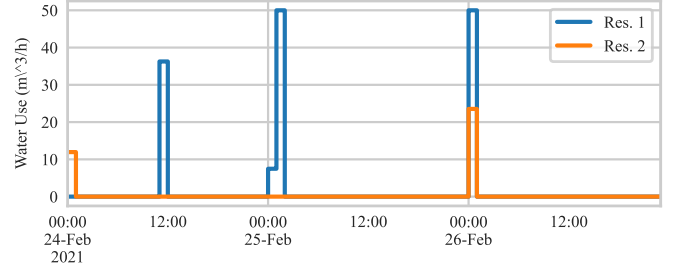Additional future work includes integration of this formula-tion with PV, load, and weather forecasts to complete the MPC or SMPC controller as well as integration with the microgrid real-time controller.

APPENDIX
LINEARIZATION FORMULATION

Some non-linear functions were linearized using auxiliary variables to create linearized versions suitable for application in a MILP solver. Details of the formulations of these are provided in this appendix. The linearized formulations generally follow the ideas from [19] but are not identical in every case.

A. max

The max function was implemented using Big M and an additional binary variable u_i for each of the input quantities a_i to the function. The binary variable u_i takes a value of 1 when a_i is the maximum input value. A new variable z is introduced as the output of the max function.

$$a_i \le z \le a_i + M(1 - u_i) \quad \forall\, i \tag{A.1}$$

$$\sum_i a_i = 1 \tag{A.2}$$

B. min

The min function was implemented by multiplying the inputs and output of the max function by –1.

$$\min(a_1, a_2, ...) = -\max(-a_1, -a_2, ...) \tag{A.3}$$

C. Absolute value

A linearized absolute value function was implemented by using Big M and introducing a new binary variable u that takes a value of 1 when the input quantity a is greater than zero. A new variable z is introduced as the output of the absolute value function.

$$-M(1-u) + a \le z \le M(1-u) + a \tag{A.4}$$
$$-Mu - a \le z \le Mu - a \tag{A.5}$$
$$z \ge 0 \tag{A.6}$$

D. Less than or equal to zero

A linearized less-than-or-equal-to-zero function was implemented by using Big M and introducing a new binary output variable z. The input quantity is a.

$$-Mz \le a \le M(1-z) \tag{A.7}$$

E. Greater than or equal to zero

A linearized greater-than-or-equal-to-zero logic function was implemented by multiplying the input to the less-than-or-equal-to logic function by −1.

$$(a \ge 0) = (-a \le 0) \tag{A.8}$$

F. Logical and

A linearized logical and function was implemented by introducing a new binary variable z for the output of the and function. The input binary values are a_1 and a_2. More than two input values were not considered in this formulation.

$$z \ge a_1 + a_2 - 1 \tag{A.9}$$
$$z \le a_i \quad \forall i \tag{A.10}$$

G. Logical or

A linearized logical or function was implemented by introducing a new binary variable z for the output of the or function. The input binary values are a_i.

$$z \ge a_i \forall i \tag{A.11}$$
$$z \le \sum_i a_i \tag{A.12}$$

REFERENCES

[1] S. Mandelli, J. Barbieri, R. Mereu, and E. Colombo, "Off-grid systems for rural electrification in developing countries: Definitions, classification and a comprehensive literature review," *Renewable and Sustainable Energy Reviews*, vol. 58, pp. 1621–1646, may 2016.

[2] M. Aliyu, G. Hassan, S. A. Said, M. U. Siddiqui, A. T. Alawami, and I. M. Elamin, "A review of solar-powered water pumping systems," pp. 61–76, may 2018.

[3] D. H. Muhsen, T. Khatib, and F. Nagi, "A review of photovoltaic water pumping system designing methods, control strategies and field performance," pp. 70–86, feb 2017.

[4] S. Chandak and P. K. Rout, "The implementation framework of a microgrid: A review," *International Journal of Energy Research*, vol. 45, no. 3, pp. 3523–3547, mar 2021.

[5] S. Choudhury, "A comprehensive review on issues, investigations, control and protection trends, technical challenges and future directions for Microgrid technology," 2020. [Online]. Available: https://doi.org/10.1002/2050-7038.12446

[6] F. A. Bhuiyan, "Optimal Sizing and Power Management Strategies of Islanded Microgrids for Remote Electrification Systems," *Thesis*, no. September, 2014. [Online]. Available: http://ir.lib.uwo.ca/etd

[7] J. Reca-Cardeña and R. López-Luque, "Design Principles of Photovoltaic Irrigation Systems," in *Advances in Renewable Energies and Power Technologies*. Elsevier, feb 2018, vol. 1, pp. 295–333.

[8] S. M. Dawoud, X. Lin, and M. I. Okba, "Hybrid renewable microgrid optimization techniques: A review," *Renewable and Sustainable Energy Reviews*, vol. 82, pp. 2039–2052, feb 2018. [Online]. Available: http://dx.doi.org/10.1016/j.rser.2017.08.007

[9] A. Ghasemi, "Coordination of pumped-storage unit and irrigation system with intermittent wind generation for intelligent energy management of an agricultural microgrid," *Energy*, vol. 142, pp. 1–13, jan 2018.

[10] A. Shoeb and G. M. Shafiullah, "Renewable Energy Integrated Islanded Microgrid for Sustainable Irrigation-A Bangladesh Perspective," *Energies*, vol. 11, no. 5, 2018. [Online]. Available: www.mdpi.com/journal/energies

[11] T. Wang, H. Kamath, and S. Willard, "Control and optimization of grid-tied photovoltaic storage systems using model predictive control," *IEEE Transactions on Smart Grid*, vol. 5, no. 2, pp. 1010–1017, mar 2014.

[12] "Güneşköy." [Online]. Available: https://www.guneskoy.org.tr/en/guneskoy/about-guneskoy-2

[13] INVT, "Goodrive100-PV Series Solar Pumping VFD Operation Manual," Tech. Rep. [Online]. Available: https://www.invt.com/uploads/file1/20200628/GD100-PVSeriesSolarPumpingVFDManual.pdf

[14] Growatt, "Off Grid Solar Inverter SPF 3500 ES SPF 5000 ES User Manual," Tech. Rep. [Online]. Available: https://www.ginverter.com/upload/file/contents/2021/09/61418e6c5e0aa.pdf

[15] U. C. Yilmaz, M. E. Sezgin, and M. Gol, "A Model Predictive Control for Microgrids Considering Battery Aging," *Journal of Modern Power Systems and Clean Energy*, vol. 8, no. 2, pp. 296–304, 2020. [Online]. Available: https://ieeexplore.ieee.org/document/8913672

[16] W. E. Hart, J.-P. Watson, and D. L. Woodruff, "Pyomo: modeling and solving mathematical programs in Python," *Mathematical Programming Computation*, vol. 3, no. 3, pp. 219–260, 2011.

[17] M. L. Bynum, G. A. Hackebeil, W. E. Hart, C. D. Laird, B. L. Nicholson, J. D. Siirola, J.-P. Watson, and D. L. Woodruff, *Pyomo–optimization modeling in python*, 3rd ed. Springer Science & Business Media, 2021, vol. 67.

[18] J. Forrest, T. Ralphs, H. G. Santos, S. Vigerske, L. Hafer, J. Forrest, B. Kristjansson, Jpfasano, EdwinStraver, M. Lubin, Rlougee, Jpgoncal1, Jan-Willem, H. i gassmann, S. Brito, Cristina, M. Saltzman, Tosttost, F. MATSUSHIMA, and To-st, "coin-or/Cbc: Release releases/2.10.7," jan 2022. [Online]. Available: https://doi.org/10.5281/zenodo.5904374

[19] "Logics and integer-programming representations - YALMIP." [Online]. Available: https://yalmip.github.io/tutorial/logicprogramming

[20] B. Chachuat, "Mixed-Integer Linear Programming (MILP): Model Formulation Mixed-Integer Linear Programming Integer Programs (IP)." [Online]. Available: http://macc.mcmaster.ca/maccfiles/chachuatnotes/07-MILP-I_handout.pdf

[21] "GNU Linear Programming Kit, Version 5.0." [Online]. Available: http://www.gnu.org/software/glpk/glpk.html

[22] A. Mesbah, "Stochastic Model Predictive Control: An Overview and Perspectives for Future Research," *IEEE Control Systems Magazine*, vol. 36, no. 6, pp. 30–44, 2016.

[23] S. Raimondi Cominesi, M. Farina, L. Giulioni, B. Picasso, and R. Scat-

tolini, "Two-layer predictive control of a micro-grid including stochastic energy sources," in *2015 American Control Conference (ACC)*, 2015, pp. 918–923.